proferriheme from analogues of compounds I and II, which in that model system are presumed to exist as mononuclear iron species.[30]

Mesoferriheme Degradation. Table IV shows the extent of heme degradation reported as % *D* as a function of heme and oxidant concentrations under various conditions. Values of % *D* are estimated from a comparison of the final recovered absorbance with the initial absorbance from stopped-flow traces, such as those shown in Figure 2.[33] Degradation increases with increasing concentrations of NaOCl in the presence of a fixed mesoferriheme concentration and decreases with increasing total (heme plus oxidant) concentration at a fixed $[mfh]_0/[OCl^-]_0$ ratio. Addition of phenol reduces the extent of degradation at relatively high hypochlorite concentrations but has a negligible effect at $[mfh]_0/[OCl^-]_0$ ratios of 1/1 or 2/1. The fact that, through peroxidatic action, phenol facilitates the regeneration of free mfh from its oxidation product suggests the species susceptible to degradation is an oxidized form of mfh rather than free heme itself, and, inasmuch as residual degradation is apparent even at low NaOCl concentrations, it appears that degradation may be signficant within the time frame of the oxidation process. The reduction in % *D* with increasing $[mfh]/[OCl^-]$ ratio also argues against degradative attack of hypochlorite on free mfh. It may be indicative, however, of competition between mfh and its oxidized form for OCl^- wherein high concentrations of free heme favor consumption of OCl^- in the *formation* of oxidized species thereby reducing the probability of degradative attack *upon* the oxidized species.[34]

Higher mfh concentrations should also facilitate comproportionation. This raises speculation that $Fe^{V}O$ may be the species most susceptible to porphyrin ring cleavage. The effect of total reactant (heme plus oxidant) concentration on % *D* at fixed $[mfh]/[OCl^-]$ ratios is not well understood; however, it is well established that the degree of heme dimerization increases with heme concentration. If dimeric heme provides a more effective "trap" for $Fe^{V}O$ than monomeric heme, e.g., via (7), then the

$$Fe^{V}O + Fe^{III}OFe^{III} \rightarrow Fe^{IV}OFe^{IV} + Fe^{III} \quad (7)$$

degree of degradation would be expected to be reduced at higher concentrations of total reactant. Figure 7 shows a linear relationship between % *D* and the ratio $[OCl^-]_0/([OCl^-]_0 + [\text{heme dimer}])$ for a series of experiments at $[mfh]_0/[OCl^-]_0 = 2/1$. Although conjectural, this is consistent with a model of competitive second-order reactions in which bimolecular attack of $Fe^{V}O$ by OCl^- and the heme dimer occurs with approximately the same probability, i.e., with similar second-order rate constants, in which case degradation would depend on the ability of oxidant to compete with free dimeric heme for $Fe^{V}O$, the mononuclear model analogue of compound I.

Molecular detail is not available with regard to the heme degradation process, but it is likely that ring fragmentation produces reducing ligands, in which case higher rates of in situ regeneration would be expected when the extent of degradation is high. At present, there are insufficient data to draw much correlation; however, it is clear that degradation of mfh exceeds that for dfh under comparable conditions, and this may be partially reflected in the relative k_2' terms for in situ regeneration. Thus, a contribution of reductant emanating from the degradation process may explain, in part, why k_2' for mfh is 20–50 times greater than the corresponding term for dfh. In terms of (6), this would be speculatively attributed to the action of the reductant on the respective dinuclear model compound II analogues.

Acknowledgment. This research was supported by the Robert A. Welch Foundation (Grant P-0162) and the TCU Research Fund.

(33) A more accurate A_0 value is obtained from an initial rate profile established by using a rapid oscilloscope scan time as described by Bretscher.[26]

(34) A thorough study of heme destruction in the coproferriheme system is described by Bretscher, who concludes "...only the cfh intermediate(s) is susceptible to destructive attack."[26]

Contribution from the Department of Chemistry,
Texas A&M University, College Station, Texas 77843-3255

New Hexaaza Macrocyclic Binucleating Ligands. Oxygen Insertion with a Dicopper(I) Schiff Base Macrocyclic Complex

Rached Menif,[†] Arthur E. Martell,* Philip J. Squattrito,[‡] and Abraham Clearfield

Received December 14, 1989

Direct 2:2 condensation of isophthalaldehyde with diethylenetriamine produces a hexaaza 24-membered macrocyclic tetra Schiff base in good yield. The crystal structure of an isomeric form of the Schiff base is reported. Crystal data for $N_6C_{24}H_{30}\cdot{}^1/_2MeOH$: $C2/c$, a = 17.283 (2) Å, b = 16.930 (2) Å, c = 17.953 (3) Å, β = 118.73 (2)°, V = 4607 (2) Å^3, Z = 8, $R(F)$ = 0.059 for 1538 observations ($I > 3\sigma(I)$) and 289 variables. The amber binuclear Cu(I) complex of the tetraaza macrocyclic Schiff base combines with a molar equivalent of dioxygen to form a green binuclear Cu(II) complex, which contains a bridging hydroxide ion and, by oxygen insertion, a bridging phenolate donor. These results provide the first macrocyclic tyrosinase model. Hydrogenation of the Schiff base provides the corresponding saturated hexaaza macrocyclic ligand. The protonation constants of the reduced macrocycle, as well as the binding constants of its mononuclear and binuclear Cu(II) complexes, have been determined potentiometrically.

Introduction

In a recent communication[1] the synthesis of a 24-membered macrocyclic tetra Schiff base, **1** (Scheme I), by a 2:2 dipodal condensation of *m*-phthaldehyde and diethylenetriamine was reported. The binuclear Cu(I) complex of this ligand, **2** (Scheme I), was found to react with dioxygen to give the corresponding binuclear Cu(II) complex, **3**, with hydroxide and ligand-derived phenoxide bridging donor groups, thus providing the first macrocyclic tyrosinase model system.

Tyrosinase and dopamine-β-hydroxylase, which insert oxygen into organic substrates, contain dinuclear Cu(I) active sites and presumably bind dioxygen as a bridging peroxo ligand between the metal centers. Karlin et al.[2] reported the first tyrosinase model, which consists of a *m*-xylyl binucleating ligand that provides two pyridine nitrogens and one aliphatic nitrogen donor to each Cu(I)

[†] Present address: Procter and Gamble Company, Brussels, Belgium.
[‡] Present address: Department of Chemistry, Central Michigan University, Mount Pleasant, MI 48859.

(1) Menif, R.; Martell, A. E. *J. Chem. Soc., Chem. Commun.* **1989**, 1522.
(2) Karlin, K. D.; Hayes, J. C.; Gultneh, Y.; Cruse, R. W.; McKown, J. W.; Hutchinson, J. P.; Zubieta, J. *J. Am. Chem. Soc.* **1984**, *106*, 2121.

0020-1669/90/1329-4723$02.50/0

Scheme I. Proposed Mechanism for the Cu(I)-Mediated Hydroxylation of a Coordinated Macrocyclic Ligand

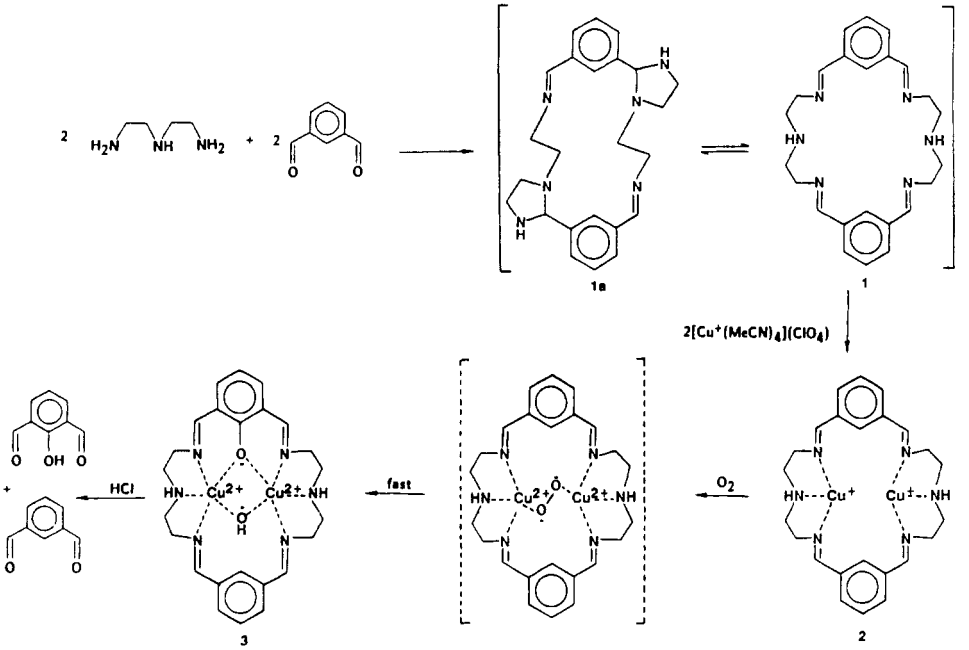

ion. Casella and Rigoni[3] described a tyrosinase model consisting of a dinuclear Cu(I) complex with one imino and one imidazole donor per metal center. Gelling et al.[4] described an analogous Schiff base model complex in which the Cu(I) ions are coordinated by an imine nitrogen and a pyridine nitrogen. The tyrosinase model system reported here is a dinuclear Cu(I) macrocyclic Schiff base complex in which the metal centers are coordinated by two imine nitrogens and one aliphatic nitrogen donor. Thus it seems that all four tyrosinase models are dinuclear Cu(I) complexes in which the soft metal ion center is coordinated by one or more soft nitrogen donors, supplied by pyridine, imidazole, Schiff base imine, or combinations of these donor groups.

This paper describes the synthesis and reactions of the new macrocyclic tyrosinase model system in greater detail than the previous communication[1] and in addition describes the crystal structure of an isomeric form of the Schiff base ligand, the $^{18}O_2$ labeling evidence for oxygen insertion, and the coordinating properties of the hexaaza 24-membered macrocyclic ligand formed by hydrogenation of the Schiff base.

Experimental Section

Materials. 3,6,9,17,20,23-Hexaazatricyclo[23.3.1.1^{11,15}]triaconta-1(29),2,9,11(30),12(13),14,16,23,25,27-decaene (1). This macrocyclic ligand was prepared by the (2 + 2) condensation of m-phthaldehyde and diethylenetriamine with the general procedure of Zagwinski et al.[5] as described previously.[1] The 200-MHz ^{1}H NMR and ^{13}C NMR spectra in $CDCl_3$ are complex, suggesting the presence of isomers of the Schiff base. Yield: 72%. Anal. Calcd for $C_{24}H_{30}N_6$: C, 71.61; H, 7.51; N, 20.88. Found (Galbraith): C, 71.33; H, 7.39; N, 20.97.

3,6,9,17,10,23-Hexaazatricyclo[23.3.1.1^{11,15}]triaconta-1(29),11-(30),12,14,25(26),27-hexaene. The saturated macrocycle **4** was obtained by hydrogenation of the Schiff base **1**, by the procedure described previously.[1] Yield: 2.11 g, 2.30 mmol, 66%. Overall yield: 48%. Anal. Calcd for $C_{24}H_{38}N_6 \cdot 6HBr$: C, 32.17; H, 4.95; N, 9.38. Found (Galbraith): C, 32.03; H, 5.09; N, 9.34. ^{1}H NMR in D_2O gave δ (ppm from TMS) 3.3–3.4 (multiplet, H of CH_2 of DIEN), 4.21 (singlet, H of CH_2 of *m*-xylyl), 7.41 (singlet, aromatic H), 7.50 (singlet, aromatic H) in the ratio of 8:4:3:1. ^{13}C NMR in $CDCl_3$ (ppm from TMS): 41.93 and 43.80 (CH_2 of DIEN), 50.93 (CH_2 of *m*-xylyl), 130.49, 130.59, 131.81, 132.01 (4 nonequivalent aromatic carbons).

Hydroxylation of 1. Two mmoles of $[Cu^I(MeCN)_4](ClO_4)$, prepared as described by van Rijn et al.,[6] was combined with 1 mmol of Schiff base (**1**, **1a**) in CH_2Cl_2 under argon. The orange dinuclear Cu(I) macrocyclic complex **2** remained stable in the absence of dioxygen. When it was exposed to dioxygen at room temperature, the color gradually turned to green. The green solid, obtained upon solvent evaporation displayed an IR band around 3500 cm^{-1}; its UV–vis absorption spectrum in MeCN has a strong absorbance at 362 (ϵ = 5800 mol^{-1}) nm as well as a weaker band near 620 nm; its solution in CD_3CN has a ^{1}H NMR resonance at 12.6 ppm from TMS. These spectral features are characteristic of phenoxo- and hydroxo-bridged binuclear copper(II) complexes **3**.

The green product was dissolved in 6 M HCl and extracted with $CHCl_3$, from which 261 mg of a yellow solid was obtained, which represents a recovery of 92%. The ^{1}H NMR spectrum of the product displayed only aromatic peaks, which showed by integration that the yellow solid was a mixture of 63% *m*-phthaldehyde and 37% 2-hydroxo-*m*-phthaldehyde, instead of the 50:50 mixture that would be obtained if the hydroxylation reaction shown in Scheme I had been complete. Thus the oxygen insertion yield found by NMR is 74% (i.e., 37/50 × 100), with only one of the arene rings hydroxylated.

$^{18}O_2$ Labeling of the Hydroxylation Product. $^{18}O_2$ (99%) was purchased from Cambridge Isotope Laboratory in 0.1-L break-seal flasks. A solution of the binuclear Schiff base macrocyclic complex **2** in acetonitrile was exposed to $^{18}O_2$. Extraction of the ligand was carried out by the method described above for oxygenation of the binuclear Cu(I) complex by $^{16}O_2$. Mass spectrometric analysis of the resulting extract gave the following peaks: *m/z* 152 (22%), 134 (100%), 133 (84%), 124 (41%). For comparison the spectrum of the extract obtained when $^{16}O_2$ was employed gave the following peaks: *m/z* 150 (56%), 134 (79%), 133 (77%), 122 (100%). Comparison of both spectra shows that the mass spectrum of the isolated 2-hydroxybenzene-1,3-dicarboxaldehyde prepared by using $^{18}O_2$ shows a shift of the 150 and 122 peaks of two mass units, indicating the incorporation of one atom of $^{18}O_2$ into the aromatic ring.

Potentiometric Determinations. Potentiometric p[H] measurements of the protonation constants and the Cu(II) binding constants of the saturated hexaaza macrocycle **4** were carried out by procedures described in detail elsewhere.[7] The measurements were made at 25.0 °C and ionic strength 0.100 M adjusted with KNO_3. The acid form of the ligand, the hexahydrobromide, was titrated with 0.1023 M carbon dioxide free standard KOH solution. The pH meter–glass electrode system was calibrated to read hydrogen ion concentration directly so that measurements provided –log [H$^+$], designated as p[H]. The log K_W value for the system, defined in terms of concentrations, log ([H$^+$][OH$^-$]), was found to be 13.78 at the ionic strength employed.

X-ray Determination of Crystal Structure of Schiff Base Ligand, $C_{24}H_{30}N_6$. A 0.1-mmol sample of **1** (40.25 mg) was dissolved in 10 mL of MeOH, and 10 mL of CH_3CN was added. The solution was allowed to evaporate slowly at room temperature over a period of 3 days. Crystals suitable for X-ray diffraction studies were obtained. A single crystal

(3) Casella, L.; Rigoni, L. *J. Chem. Soc., Chem. Commun.* **1985**, 1668.
(4) Gelling, O. J.; van Bolhuis, F.; Meetsma, A.; Feringa, B. L. *J. Chem. Soc., Chem. Commun.* **1988**, 552.
(5) Zagwinski, J.; Lehn, J. M.; Meric, R.; Vigneron, J. P. *Tetrahedron Lett.* **1987**, *28*, 3489.
(6) van Rijn, J.; Reedijk, J.; Dartmann, M.; Kregs, B. *J. Chem. Soc., Dalton Trans.* **1987**, 2579.
(7) Martell, A. E.; Motekaitis, R. J. *The Determination and Use of Stability Constants*; VCH Publishers: New York; 1989.

Table I. Summary of Crystallographic Data for $C_{24}H_{30}N_6 \cdot {}^1/_2CH_3OH$

fw	418.57
a, Å	17.283 (2)
b, Å	16.930 (2)
c, Å	17.953 (3)
β, deg	118.73 (2)
V, Å^3	4607 (2)
space group	$C2/c$ (No. 15)
Z	8
D_{calc}, g/cm^3	1.207
μ(Mo Kα), cm^{-1}	0.67
diffractometer	Rigaku AFC5R
radiation	Mo Kα (λ = 0.710 69 Å) (graphite monochromated)
temp, °C	23 ± 1
R(F)	0.059
R_w(F)	0.074
error in observn of unit wt	1.76
max, min peaks in final Δf	+0.17, −0.22

mounted on a glass fiber was placed on a Rigaku AFC5R four-circle diffractometer equipped with a 12-kW rotating anode Mo X-ray source (graphite-monochromated Kα, λ = 0.710 69 Å). Indexing of 25 reflections found in a search of reciprocal space followed by cell reduction by the program XCELL[8] resulted in the monoclinic C-centered cell given in Table I. Accurate unit cell parameters were obtained at room temperature from a least-squares analysis of the setting angles of 22 high-angle reflections (25° < 2θ (Mo Kα) < 37°). Intensity data were collected by using the ω-2θ scan technique and a scan speed of 16 deg min^{-1} in ω in the 2θ angular range 2–50°. Weak reflections were scanned up to three times and counts accumulated for good count statistics. The intensities of three standard reflections, monitored by 150 reflection intervals throughout the data collection, showed no significant fluctuations or decay. No absorption correction was performed. The space group was assigned as $C2/c$ on the basis of intensity statistics and systematic absences ($h0l$: $h, l \neq 2n$) and (hkl: $h + k \neq 2n$). A total of 4514 reflections were scanned of which 1538 were unique with $I > 3.00\sigma(I)$. Structure solution and refinement was performed on a DEC MicroVAX II computer with the TEXSAN[9] series of programs. The structure was solved by direct methods. The asymmetric unit contains half of each of the two independent but essentially identical molecules that occupy the unit cell. Parts of both molecules were evident on an E map calculated by the program MITHRIL.[10] The remaining non-hydrogen atoms were found on successive electron density maps calculated by using direct-method phase-refinement techniques (DIRDIF[11]). Hydrogen atoms were found on difference electron density maps and were included in subsequent refinements as fixed isotropic scatterers. The difference maps also revealed two closely spaced peaks of roughly the same height located near an inversion center in between the $C_{24}H_{30}N_6$ molecules. These peaks were included in the model at a fixed occupancy of 50% as a disordered methanol molecule. The final refinement was performed on those data for which $I > 3\sigma(I)$ and included anisotropic thermal parameters for all non-hydrogen atoms. The final cycle of full-matrix least-squares refinement was based on 1538 reflections, and 289 variable parameters converged with unweighted and weighed agreement factors $R(F) = \sum||F_o| - |F_c|/\sum|F_o| = 0.059$ and $R_w(F) = [\sum w(|F_o| - |F_c|)^2/\sum wF_o^2]^{1/2} = 0.074$. An analysis of F_o vs F_c as a function of (sin θ)/λ, Miller indices, and F_o displayed no unusual trends. The extreme peaks in the final difference Fourier map are +0.17 and −0.22. Details of the X-ray experiment and crystal data are summarized in Table I.

Results

Synthesis. The synthetic pathway to the binuclear Cu(I) hexaaza macrocyclic (tetra Schiff base) complex and eventually to the corresponding binuclear Cu(II) complex is illustrated in Scheme I. The nontemplate procedure for forming the macrocyclic ligand is straightforward and gives a high yield of product. This one-step synthesis is very efficient, and the product may also be hydrogenated in high yield to produce the reduced hexaaza binuclear macrocyclic ligand, also in excellent yield. The procedures described in the Experimental Section therefore represent a highly efficient synthesis of both the unsaturated and saturated macrocycles. As indicated in Scheme I, the tetra Schiff base may be readily hydrolyzed to aldehyde and polyamine to facilitate examination of the ligand for possible hydroxylation reactions promoted by dioxygen complex formation.

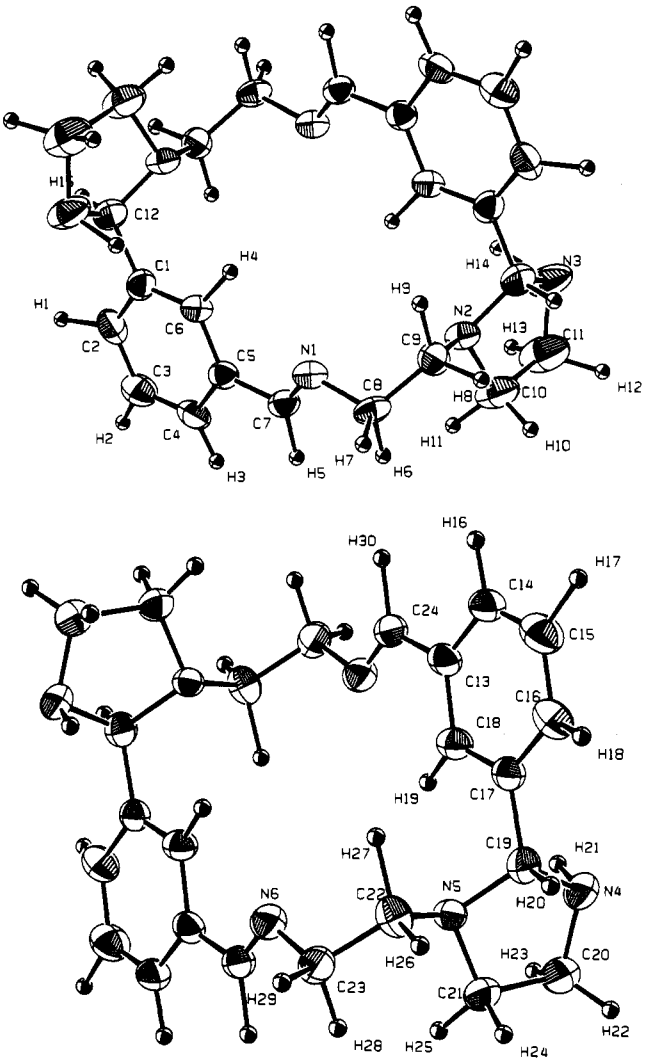

Figure 1. Structural views of molecules A (top) and B (bottom) together with the atomic numbering schemes.

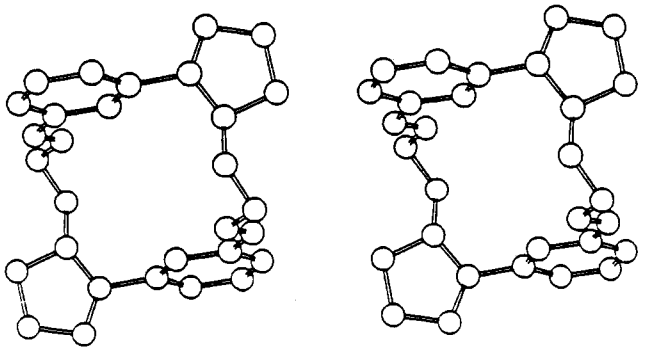

Figure 2. Stereoview of molecule A.

Structure of $C_{24}H_{30}N_6 \cdot {}^1/_2$MeOH, the Hexaaza Macrocyclic Schiff base (1). The ligand crystallized from solution consists of the macrocycle $C_{24}H_{30}N_6$ and $^1/_2$ equiv of a methanol molecule, with the solvent molecule of crystallization MeOH located between two ligand molecules. The ligand crystallized in the monoclinic space group $C2/c$ and possesses a center of inversion. There are

(8) Sheldrick, B. M. *SHELXTL-PLUS*, Nicolet Instrument Corp.: Madison, WI, 1988 (revision 3.4).
(9) *TEXSAN, Texray Structural Analysis Package*; Molecular Structure Corp.: The Woodlands, TX, 1987 (revised).
(10) Gilmore, G. J. MITHRIL: A Computer Program for the Automatic Solution of Crystal Structures from X-ray Data. University of Glasgow, Scotland, 1983.
(11) Beurkens, P. T.; DIRDIF: Direct Methods for Difference Structures—An Automatic Procedure for Phase Extension and Refinement of Difference Structure Factors. Technical Report 1984/1; Crystallography Laboratory: Toernooiveld, 6525 Ed Nijmegen, The Netherlands.

Table II. Positional and Equivalent Isotropic Thermal Parameters for $C_{24}H_{30}N_6 \cdot {}^1/_2MeOH$

atom	x	y	z	B_{eq},[a] Å^2
N1A	−0.0250 (3)	0.0903 (3)	0.1057 (3)	4.1 (2)
N2A	0.0273 (3)	0.1969 (3)	0.0044 (3)	4.2 (2)
N3A	0.1045 (5)	0.2263 (4)	−0.0685 (5)	8.2 (2)
C1A	0.0376 (4)	−0.1548 (4)	0.1468 (4)	4.5 (3)
C2A	0.1048 (5)	−0.1779 (4)	0.2285 (5)	5.2 (3)
C3A	0.1496 (4)	−0.1206 (5)	0.2890 (4)	5.6 (4)
C4A	0.1304 (4)	−0.0421 (5)	0.2708 (4)	4.9 (3)
C5A	0.0632 (4)	−0.0191 (4)	0.1902 (4)	3.8 (3)
C6A	0.0180 (4)	−0.0768 (4)	0.1284 (4)	3.9 (3)
C7A	0.0406 (4)	0.0656 (4)	0.1717 (4)	4.0 (3)
C8A	−0.0399 (4)	0.1754 (4)	0.0962 (4)	4.5 (3)
C9A	−0.0529 (4)	0.2040 (3)	0.0127 (4)	4.3 (3)
C10A	0.0982 (5)	0.2503 (4)	0.0608 (5)	6.8 (4)
C11A	0.1576 (5)	0.2580 (5)	0.0190 (6)	8.8 (5)
C12A	0.0141 (5)	0.2171 (4)	−0.0805 (4)	5.4 (3)
H1A	0.1241	−0.2428	0.2601	6.1
H2A	0.2018	−0.1316	0.3510	6.4
H3A	0.1646	0.0027	0.3137	5.6
H4A	−0.0272	−0.0539	0.0594	4.6
H5A	0.0896	0.1002	0.2316	4.4
H6A	0.0157	0.2007	0.1507	5.4
H7A	−0.0884	0.2002	0.1113	5.4
H8A	−0.0727	0.2653	−0.0023	5.1
H9A	−0.0976	0.1677	−0.0429	5.1
H10A	0.0758	0.3102	0.0671	8.4
H11A	0.1264	0.2222	0.1262	8.4
H12A	0.1540	0.3267	0.0007.	11.2
H13A	0.2287	0.2055	0.0563	11.2
H14A	0.1291	0.1487	−0.0616	9.8
H15A	−0.0210	0.2718	−0.0933	6.5
N1B	0.6788 (4)	0.2466 (3)	−0.1632 (3)	4.6 (2)
N2B	0.7088 (3)	0.0783 (3)	−0.1043)3)	3.4 (2)
N3B	0.7811 (4)	−0.0298 (3)	−0.0176 (3)	5.3 (3)
C1B	0.6849 (4)	0.0500 (4)	0.0197 (4)	3.8 (3)
C2B	0.6306 (4)	0.0093 (4)	0.0442 (4)	4.9 (3)
C3B	0.6206 (5)	0.0376 (5)	0.1121 (5)	5.7 (4)
C4B	0.6652 (5)	0.1057 (4)	0.1559 (4)	4.9 (3)
C5B	0.7184 (4)	0.1462 (4)	0.1311 (4)	4.0 (3)
C6B	0.7273 (4)	0.1184 (4)	0.0616 (4)	4.0 (3)
C7B	0.7358 (4)	0.2816 (4)	−0.1763 (4)	4.1 (3)
C8B	0.6347 (4)	0.1782 (4)	−0.2149 (4)	4.9 (3)
C9B	0.6247 (4)	0.1130 (4)	−0.1623 (3)	4.3 (3)
C10B	0.7516 (4)	0.0375 (4)	−0.1465 (4)	4.6 (3)
C11B	0.8131 (5)	−0.0235 (4)	−0.0811 (4)	5.6 (3)
C12B	0.6983 (4)	0.0168 (4)	−0.0520 (4)	4.2 (3)
H1B	0.5787	−0.0307	0.0032	5.6
H2B	0.5703	0.0057	0.1352	6.9
H3B	0.6515	0.1291	0.2043	6.0
H4B	0.7820	0.1480	0.0524	4.9
H5B	0.7616	0.2607	−0.2269	4.9
H6B	0.6701	0.1514	−0.2478	5.9
H7B	0.5598	0.1881	−0.2751	5.9
H8B	0.5742	0.0712	−0.2091	5.6
H9B	0.6026	0.1437	−0.1087	5.6
H10B	0.7067	−0.0011	−0.2010	5.6
H11B	0.7754	0.0757	−0.1763	5.6
H12B	0.7977	−0.0827	−0.1104	7.4
H13B	0.8775	0.0153	−0.0491	7.4
H14B	0.8336	0.0091	0.0318	6.4
H15B	0.6445	−0.0231	−0.0945	5.1
O1S	0.3509 (9)	0.1626 (6)	0.1461 (8)	10.3 (7)
C1S	0.445 (1)	0.134 (1)	0.210 (1)	24 (2)

[a] $B_{eq} = {}^4/_3[a^2\beta_{11} + b^2\beta_{22} + c^2\beta_{33} + (2ab\cos\gamma)\beta_{12} + (2ac\cos\beta)\beta_{13} + (2bc\cos\alpha)\beta_{23}]$.

two crystallographically independent macrocycles: molecule A and molecule B (Figure 1). Each unit cell contains four macrocycles, two of each type. The closest intermolecular contacts are those between H atoms (H7A–H4B, 2.16 Å; H4A–H13B, 2.19 Å) and between N and H atoms (N1B–H7A, 2.35 Å). Positional and equivalent isotropic thermal parameters obtained for all atoms in the structure are given in Table II. The macrocycle contains an 18-membered inner ring, two imine bonds, and two 5-membered imidazolidine outer rings. Selected bond distances and angles for

Table III. Intramolecular Distances (Å) Involving the Non-Hydrogen Atoms

N1A–C7A	1.254 (7)	N1B–C7B	1.264 (7)
N1A–C8A	1.459 (7)	N1B–C8B	1.450 (8)
N2A–C10A	1.467 (8)	N2B–C10B	1.463 (7)
N2A–C9A	1.468 (7)	N2B–C9B	1.445 (6)
N2A–C12A	1.469 (8)	N2B–C12B	1.470 (7)
N3A–C12A	1.479 (8)	N3B–C12B	1.485 (7)
N3A–C11A	1.49 (1)	N3B–C11B	1.490 (8)
C1A–C6A	1.365 (8)	C1B–C6B	1.384 (8)
C1A–C2A	1.421 (8)	C1B–C2B	1.394 (8)
C1A–C12A	1.518 (9)	C1B–C12B	1.520 (8)
C2A–C3A	1.38 (1)	C2B–C3B	1.396 (9)
C3A–C4A	1.371 (9)	C3B–C4B	1.400 (9)
C4A–C5A	1.406 (8)	C4B–C5B	1.380 (8)
C5A–C6A	1.400 (8)	C5B–C6B	1.411 (8)
C5A–C7A	1.482 (8)	C5B–C7B	1.470 (8)
C8A–C9A	1.486 (8)	C8B–C9B	1.516 (8)
C10A–C11A	1.54 (1)	C10B–C11B	1.541 (8)
O1S–C1S	1.54 (2)		

Table IV. Intramolecular Bond Angles (deg) Involving the Non-Hydrogen Atoms

C7A–N1A–C8A	118.0 (5)	C7B–N1B–C8B	118.2 (6)
C10A–N2A–C9A	113.3 (5)	C10B–N2B–C9B	113.7 (4)
C10A–N2A–C12A	103.6 (5)	C10B–N2B–C12B	104.2 (5)
C9A–N2A–C12A	113.8 (5)	C9B–N2B–C12B	111.0 (4)
C12A–N3A–C11A	105.4 (5)	C12B–N3B–C11B	106.4 (5)
C6A–C1A–C2A	120.1 (6)	C6B–C1B–C2B	120.2 (6)
C6A–C1A–C12A	119.9 (6)	C6B–C1B–C12B	120.8 (6)
C2A–C1A–C12A	120.0 (6)	C2B–C1B–C12B	119.0 (6)
C3A–C2A–C1A	119.4 (6)	C3B–C2B–C1B	119.4 (6)
C4A–C3A–C2A	120.8 (6)	C4B–C3B–C2B	120.5 (6)
C3A–C4A–C5A	120.0 (6)	C3B–C4B–C5B	120.0 (6)
C6A–C5A–C4A	119.6 (6)	C6B–C5B–C4B	119.6 (6)
C6A–C5A–C7A	120.7 (5)	C6B–C5B–C7B	120.4 (6)
C4A–C5A–C7A	119.8 (6)	C4B–C5B–C7B	120.1 (6)
C1A–C6A–C5A	120.2 (6)	C1B–C6B–C5B	120.4 (6)
N1A–C7A–C5A	123.8 (6)	N1B–C7B–C5B	123.3 (6)
N1A–C8A–C9A	111.9 (5)	N1B–C8B–C9B	111.4 (5)
N2A–C9A–C8A	112.6 (5)	N2B–C9B–C8B	111.7 (5)
N2A–C10A–C11A	104.3 (6)	N2B–C10B–C11B	104.9 (5)
N3A–C11A–C10A	105.4 (6)	N3B–C11B–C10B	104.9 (5)
N2A–C12A–N3A	104.3 (6)	N2B–C12B–N3B	104.6 (5)
N2A–C12A–C1A	113.0 (5)	N2B–C12B–C1B	113.3 (5)
N3A–C12A–C1A	111.7 (5)	N3B–C12B–C1B	110.7 (5)

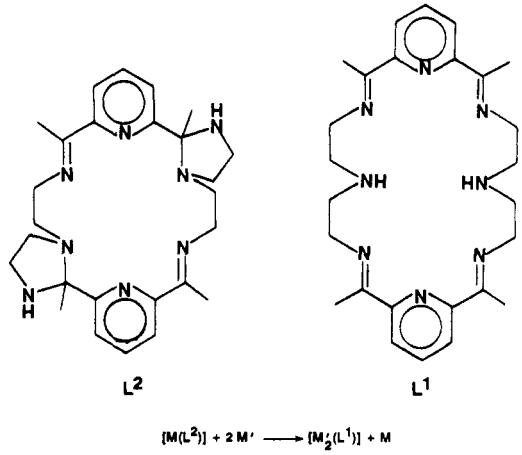

Figure 3. "Trans-bimetalation"-induced expansion of an 18-membered diimine diimiazolidine macrocyclic complex.[20]

the two independent molecules are provided in Tables III and IV. ORTEP views as well as numbering of the atoms are given in Figure 1 for molecules A and B. Each macrocycle contains two coplanar aromatic ring systems and two coplanar five-membered imidazolidine rings. The aromatic rings are approximately perpendicular to the aliphatic rings as shown in Figure 2. Bond lengths and angles in the macrocycles are normal, with no remarkable differences between molecules A and B. We do note some small but

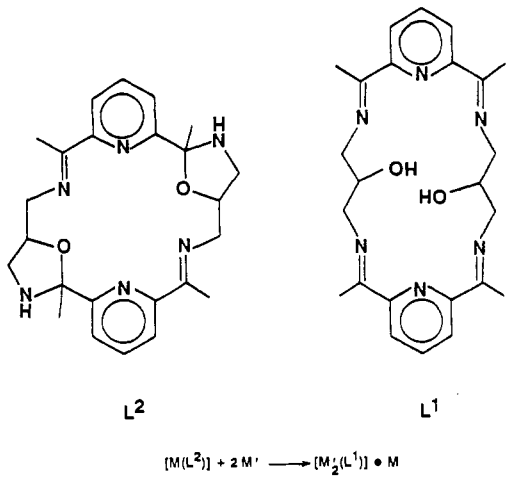

Figure 4. Trans-bimetalation-induced expansion of an 18-membered diimine dioxazolidine macrocyclic complex.[21]

significant variations in torsion angles about the bonds to the aromatic rings: N1–C7–C5–C6, A = 9 (1)°, B = 40.1 (5)°; C1′–C12–N2–C9, A = −91.3 (5)°, B = −77.1 (6)°; N2–C12–C1′–C6′, A = −14.5 (5)°, B = −35.4 (8)°.

Isomerization of MX_2DIEN_2. The product prepared by the (2 + 2) Schiff base condensation of diethylenetriamine and *m*-phthalaldehyde gave an elemental analysis in satisfactory agreement with the chemical formula $C_{24}H_{30}N_6$. However, the 200-MHz ^1H NMR and ^{13}C NMR spectra in $CDCl_3$ were complex, suggesting that the product of the condensation was probably a mixture of isomers. The structure of one of the isomers was revealed by a single-crystal X-ray structure determination using crystals grown from a solution obtained by dissolution of the condensation product in MeOH–MeCN. The most significant finding is that the crystallized product has the structure shown in Figure 1 (formula **1a** in Scheme I), containing an 18-membered macrocycle, rather than the expected complex, **1**, having a 24-membered inner ring.

Oxygen Insertion. In the presence of 2 equiv of copper(I) ion, the equilibrium between the two forms in the isomeric mixture **1** and **1a** is probably completely shifted to the right (Scheme I), the 24-membered macrocyclic isomeric form being able to provide the donor sites needed to accommodate two metal ions. Thus the macrocyclic ligand of the binuclear complex **2** has the conformation indicated by **1**. When **2** was exposed to dioxygen at room temperature, the aromatic ring was rapidly hydroxylated, and spectroscopic evidence (reported in the Experimental) points toward the formation of the (μ-hydroxy)(μ-phenoxy)dicopper(II) complex **3** (Scheme I). The green compound **3** was dissolved in 6 M HCl and extracted with $CHCl_3$. A thorough analysis of the ^1H NMR spectral data of the organic phase extract shows clearly that hydroxylation had occurred at the 2-position of the phenyl ring (Figure 5).

An experiment under identical conditions with $Co(ClO_4)_2$ as a metal source instead of $[Cu^I(MeCN)_4](ClO_4)$ was carried out. After exposure to dioxygen, the same procedure as that described for the isolation of the aromatic part of the ligand in the Cu(I) studies was employed. The ^1H NMR spectrum of the extract from the organic phase was clearly identified as that of isophthaldehyde, and the extraction yield was 96%. Therefore, it was concluded that oxygen insertion parallel to that which occurs with the Cu(I) binuclear Schiff base complex cannot be duplicated when Cu(I) is replaced by Co(II).

Table V. Protonation Constants and Cu(II) Binding Constants of the Hexaaza Macrocyclic Ligand L (**4**)

symbol	equilibrium quotient	log K_y^a
K_1^H	$[HL]/[H][L]$	9.49
K_2^H	$[H_2L]/[H][HL]$	8.73
K_3^H	$[H_3L]/[H][H_2L]$	8.03
K_4^H	$[H_4L]/[H][H_3L]$	7.29
K_5^H	$[H_5L]/[H][H_4L]$	3.64
K_6^H	$[H_6L]/[H][H_5L]$	3.45
K_{ML}^M	$[ML]/[M][L]$	13.79
K_{MHL}^H	$[MHL]/[H][ML]$	8.69
$K_{MH_2L}^H$	$[MH_2L]/[H][MHL]$	7.32
$K_{M_2L}^M$	$[M_2L]/[M][ML]$	9.68
$K_{M_2(OH)L}^{OH}$	$[M_2(OH)L][H]/[M_2L]$	−7.26
$K_{M_2(OH)_2L}^{OH}$	$[M_2(OH)_2L][H]/[M_2(OH)L]$	−8.40

[a] 25.0 °C, μ = 0.100 M (KNO_3).

Metal Complex Stability Studies on the Hexaaza Macrocycle $C_{24}H_{38}N_6$ (4). The potentiometric investigation of the protonation constants and Cu(II) binding constants of the reduced hexaaza macrocyclic ligand **4**, carried out as described in the Experimental Section, produced the p[H] profile in Figure 6. The equilibrium constants obtained from the data in Figure 6 are presented in Table V. The p[H] profile of the ligand has a 4-equiv buffer region for p[H] 7–10, indicating the presence of four moderately to

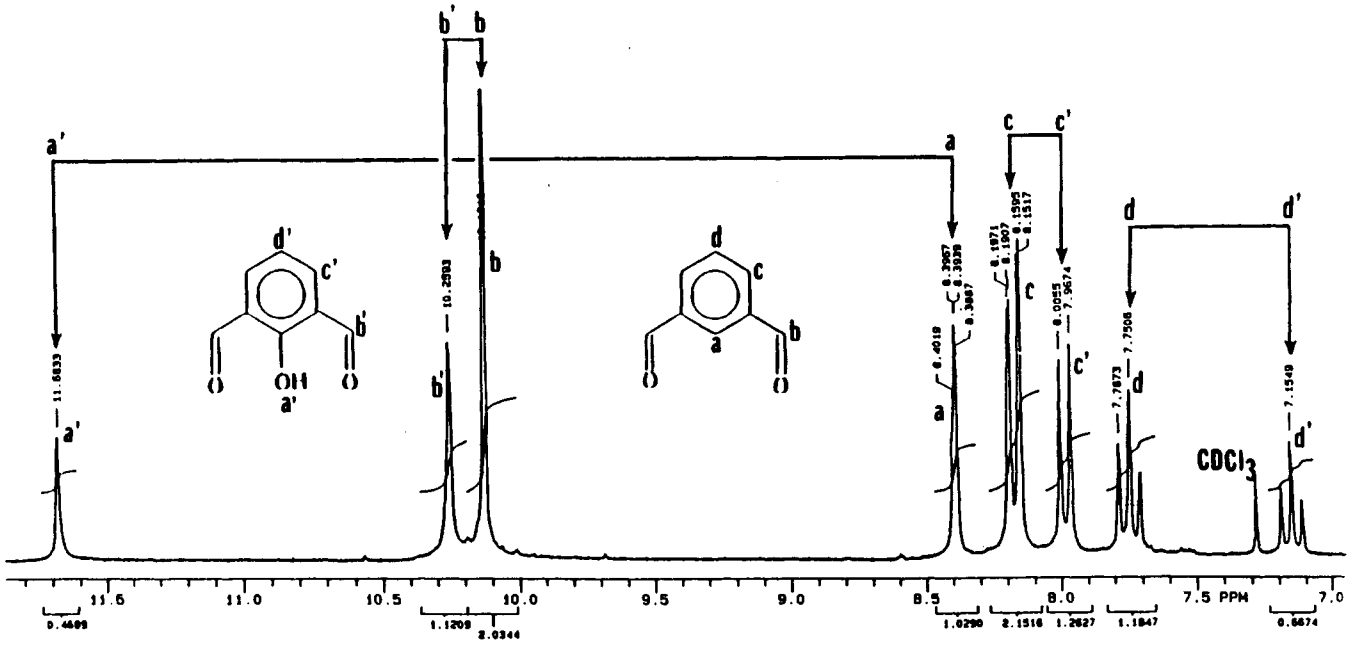

Figure 5. ^1H NMR spectrum of the organic extract of the hydroxylation product of the binuclear Cu(I) complex **2** of the hexaaza macrocyclic tetra Schiff base. Spectrum was recorded in $CDCl_3$ relative to TMS.

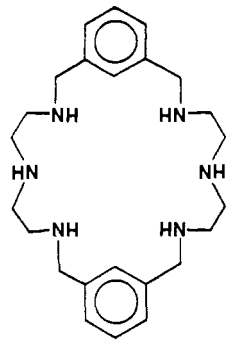

4 Hexaaza macrocyclic ligand

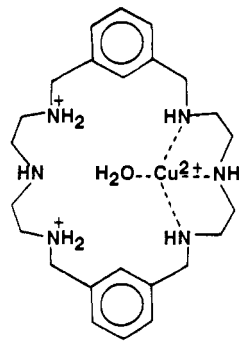

5 Diprotonated mononuclear Cu(II) complex of 4

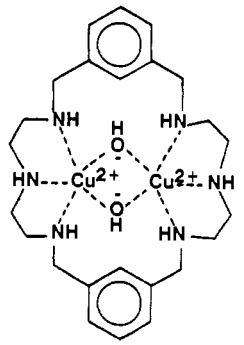

6 Dihydroxo bridged dinuclear Cu(II) complex of 4

strongly basic amino nitrogens. The remaining two amine groups have low basicity, as indicated by the ligand curve in Figure 6. It is clear that the weakly basic nitrogens are the central amino groups of the diethylenetriamine moieties in the macrocycle, strongly influenced by the coulombic effects of two adjacent (positive) protonated amino groups. These qualitative observations are in agreement with the calculated protonation constants in Table V.

The Cu(II) curves in Figure 6 show that both mononuclear (1:1) and binuclear (2:1) complexes are formed. The mononuclear complex CuL^{2+} (L = **4**) forms two protonated complexes $CuHL^{3+}$ and CuH_2L^{4+}, indicating that the metal ion is coordinated to one diethylenetriamine moiety, leaving the other free for protonation. A probable coordinate bonding arrangement for the diprotonated mononuclear complex is indicated by **5**. The binuclear complex Cu_2L^{4+} is characterized by strong hydrolytic tendencies to form mono- and dihydroxo complexes. In accordance with analogous studies on binuclear complexes of BISDIEN.[12] It is suggested that the hydroxide ions are bridging groups coordinated simultaneously to both metal ions, as indicated by **6**.

Discussion

Synthesis. The synthesis of macrocyclic Schiff bases by metal-free condensations of primary di- or triamines with dialdehydes is a relatively new reaction, and only a few examples have been published previously. The first reports were published by Tasker et al.[13] and Fenton et al.[14] Additional examples were subsequently reported by Moore et al.,[15] Zagwinski et al.,[5] MacDowell and Nelson,[16] Drew et al.,[17] and Fenton et al.[18] High yields seem to be the norm with isophthaldehyde condensations.[19]

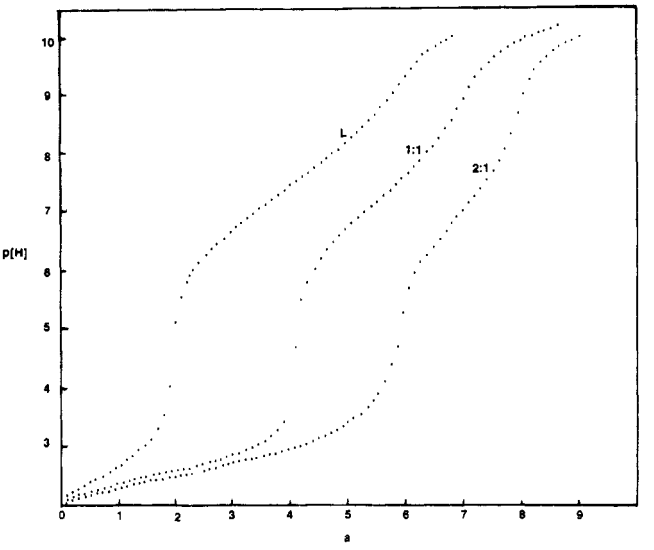

Figure 6. p[H] profiles of the hexahydrobromide of hexaazamacrocycle **4**, $C_{24}H_{38}N_6 \cdot 6HBr$, L, and for 1:1 and 2:1 molar ratios of Cu(II) to ligand. Concentration of ligand = 1.00×10^{-3} M, t = 25.0 °C, μ = 0.100 M (KNO_3). Points indicate individual experimental measurements of p[H]; a = moles of base (KOH) added per mole of ligand.

Hydrogenation of the Schiff bases produces the corresponding saturated binucleating polyaza macrocyclic and cryptand ligands, thus opening up a facile route for the synthesis of an extensive series of ligands and their binuclear metal complexes. This new synthetic method was employed in this research for the condensation of *m*-phthaldehyde with diethylenetriamine to produce, in a single step, the macrocyclic tetra Schiff base complex **1** in 72% yield. This is an exceptionally high yield for a dipodal (2 + 2) reaction and is considerably higher than the range of yields reported previously[16] for cyclic Schiff base condensations. As a rationalization of why cyclic condensation predominates so strongly over the normally expected linear condensation to produce polymeric Schiff bases, it is suggested that the cyclic product is thermodynamically preferred over the polymer and that the long period of time allowed for the reaction makes possible the redistribution of Schiff base species from the oligomers (which may be kinetically favored) to the more thermodynamically stable cyclic Schiff bases. It should be noted that such rearrangement is made possible by the labile nature of the Schiff bases formed in solution and their ability to interconvert to one another. It should be further noted that the high yield in this synthesis was achieved without the use of a metal ion as a template for the condensation.

Isomerism of MX_2DIEN_2. The [24] → [18] ring contraction (Scheme I) can thus be seen as a consequence of the nucleophilic addition of the two secondary amine functions of **1** across adjacent imine bonds to give **1a**. Two closely related examples of such inner-ring contractions were reported by Drew et al.[20] and Adams et al.,[21] respectively. In both cases, a contraction ([24] → [18]) was observed during the template (2 + 2) condensation reaction of diamine and dialdehyde, and it was proposed that the condensation is induced by the template metal ion. Internal nucleophilic addition of two secondary amine or alcohol functions of the lateral units across adjacent imine bonds led to the formation of two imidazolidine or oxazolidine rings. In both cases, it was reported[20,21] that trans bimetalation of the mononuclear complex to a disilver(I) or dicopper(II) complex occurred with ring expansion (Figures 3 and 4). They also found that reduction of the mononuclear 18-membered macrocyclic complex with metal hydride resulted in the formation of the corresponding 24-membered polyamine macrocyclic complex. Similarly, as reported in the

(12) Motekaitis, R. J.; Martell, A. E.; Lecomte, J. P.; Lehn, J. M. *Inorg. Chem.* **1983**, *22*, 609.
(13) Owston, P. G.; Peters, R.; Ramsammy, E.; Tasker, P. A.; Trotter, J. *J. Chem. Soc., Chem. Commun.* **1980**, 1218.
(14) Bailey, N. A.; Eddy, M. M.; Fenton, D. E.; Jones, G.; Moss, S.; Mukhopadhyay, A. *J. Chem. Soc., Chem. Commun.* **1981**, 628.
(15) Alcock, N. W.; Kingston, R. G.; Moore, P.; Pierpoint, C. *J. Chem. Soc., Dalton Trans.* **1984**, 1937.
(16) MacDowell, D.; Nelson, J. *Tetrahedron Lett.* **1988**, *29*, 385.
(17) Drew, M. G. B.; MacDowell, D.; Nelson, J. *Polyhedron* **1988**, *7*, 2229.
(18) Bailey, N. A.; Fenton, D. E.; Williams, M. G.; Winter, D. J. *J. Chem. Soc., Dalton Trans.* **1989**, 1727.
(19) McKee, V.; Robinson, W. T.; McDowell, D.; Nelson, J. *Tetrahedron Lett.* **1989**, *30*, 7453.
(20) Drew, M.; Nelson, J.; Nelson, S. M. *J. Chem. Soc.*, Dalton *Trans.* **1981**, 1678.
(21) Adams, H.; Bailey, N. A.; Fenton, D. E.; Good, R. J.; Moody, R.; Cecilia, O.; de Barbarin, R. *J. Chem. Soc., Dalton Trans.* **1988**, 207.

Experimental Section, treatment of the condensation product with $NaBH_4$ resulted in reduction of the two imine bonds and ring opening of the two imidazolidine five-membered rings. It is noted, however, that in the present research metal ions were not involved in ring contraction and expansion.

It is proposed that the condensation product is a mixture of 18-membered and 24-membered macrocycles and that, under the crystallization conditions, the 18-membered macrocycle crystallizes more readily. In solution, an equilibrium between the two isomeric forms is postulated as shown in Scheme I.

Oxygen Insertion. A plausible hydroxylation mechanism is indicated by Scheme I. An essential part of this mechanism is the activation of dioxygen through the formation of a very short-lived intermediate dioxygen complex of **2**, which is rapidly converted with concomitant oxygen insertion to the hydroxo- and phenoxo-bridged macrocyclic binuclear Cu(II) complex **3**.

Further support for the proposed mechanism was provided by carrying out a parallel oxygenation experiment with $^{18}O_2$ as the source of dioxygen. The mass spectrum of the 2-hydroxybenzene-1,3-dicarboxaldehyde isolated from the reaction mixture as described in the Experimental Section showed an increase of two mass units for the two most intense peaks compared to the mass spectrum obtained by oxygenation with $^{16}O_2$. Thus it is clear that the oxygen inserted into the ligand in the hydroxylation reaction is derived from the molecular oxygen supplied to the binuclear Cu(I) complex **2**.

These results demonstrate the synthesis of the first macrocyclic tyrosinase model and show that an open-chain binucleating ligand is not a prerequisite. The results are also in agreement with the suggestion by Gelling et al.[4] that the nature of the donor groups (i.e., imine, aromatic amine, aliphatic amine) and the number of donor atoms per Cu(I) (i.e., two or three) are not critical. Probably, the key factors in designating a successful tyrosinase model are the total basicity of the Cu(I) donor groups (which should be low) and the positioning of the two copper(I) ions with respect to each other and to the aromatic C–H bond. The failure of cobalt(II) to mediate the hydroxylation of the macrocycle MX_2DIEN_2 is indicative that the nature of the metal ion is an important factor.

Degradation of Co(II) and Cu(I) Dioxygen Complexes. It is noteworthy that the dinuclear cobalt(II) dioxygen complex of the hexaaza macrocyclic complex does not promote hydroxylation of the benzene rings in the bridging groups between the diethylenetriamine coordinating moieties. This result is in sharp contrast to the reactivity of the corresponding dinuclear Cu(I)) dioxygen complex of the binucleating hexaaza tetra Schiff base ligand that undergoes very rapid aromatic hydroxylation. Although the oxygenation constant could not be determined potentiometrically because of the rapid degradation of the complex, its thermodynamic stability is estimated to be similar in magnitude to that of the dicobalt(II)–BISDIEN complex, with a $P_{1/2}^{-1}$ of about 2×10^5 atm^{-1} at pH 7 in aqueous solution. This high thermodynamic stability is similar to those of many other cobalt(II) polyamine complexes. It is interesting that thus far none of these complexes have been observed to promote hydroxylation reactions, but rather undergo metal-centered degradation to the corresponding inert Co(III) complexes with the release of hydrogen peroxide.[22] It is now suggested that the high thermodynamic stability is an indication of extensive electron transfer from the cobalt(II) to the dioxygen, so that the complex, which is usually written as two cobalt(III) centers coordinated to a bridging peroxo group, has charge distribution close to that of the extreme bond structure Co^{3+}–O^-–O^-–Co^{3+}. Thus it is reasonable to expect that the lowest energy pathway to inert products is completion of the transfer, accompanied by concomitant facile protonation (in aqueous solution) of the peroxo bridge, releasing hydrogen peroxide.

It is suggested that this process cannot occur as readily in the dicopper(I)–dioxygen system for two reasons—the absence of water in the acetonitrile solvent and the lower degree of electron transfer from the metal ion to the bridging dioxygen in the dioxygen complex. This lower degree of electron transfer is reasonable because of the presence of the four weakly basic imine donors (two per metal ion) in the ligand, resulting in lower thermodynamic stability of the dioxygen complex. The mechanism suggested for oxygen insertion by this complex is one that conserves the hydrogen at the hydroxylation site for formation of the second (hydroxyl) bridging group, as follows:

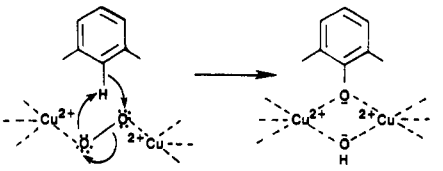

Because of the proximity of the coordinated dioxygen to the hydroxyl site, a concerted electron-transfer process seems reasonable.

The fact that the corresponding dinuclear Co(II) complex of the same ligand does not catalyze hydroxylation, as described above, is somewhat surprising, in view of the weak coordination tendency of the imine donor groups. It is planned to investigate the possibility of this reaction further, with the use of bridging groups containing more active C–H sites through substitution of the para positions with electron-releasing substitutents.

Acknowledgment. This research was supported by L'Air Liquide, S.A., and by a research contract from the Office of Naval Research. R.M. acknowledges with thanks a Convention Cifre Scholarship from the French Ministry of Research and Technology. The contributions of P.J.S. and A.C. were supported by a grant, A673, from the Robert A. Welch Foundation.

Supplementary Material Available: A table of anisotropic thermal parameters (2 pages); a table of structure factors (31 pages). Ordering information is given on any current masthead page.

(22) Martell, A. E. In *Oxygen Complexes and Oxygen Activation by Transition Metals*; Martell, A. E., Sawyer, D. T., Eds.; Plenum: New York, 1988; pp 87–106.